Chemosphere 312 (2023) 137138

Contents lists available at ScienceDirect

Chemosphere

journal homepage: www.elsevier.com/locate/chemosphere

Interactions of airborne graphene oxides with the sexual reproduction of a model plant: When production impurities matter

Davide Zanelli [a], Fabio Candotto Carniel [a,*], Lorenzo Fortuna [b], Elena Pavoni [c], Viviana Jehová González [d], Ester Vázquez [d,e], Maurizio Prato [f,g,h], Mauro Tretiach [a]

[a] Department of Life Sciences, University of Trieste, 34127, Trieste, Italy
[b] Department of Engineering and Architecture, University of Trieste, 34127, Trieste, Italy
[c] Department of Mathematics and Geosciences, University of Trieste, 34128, Trieste, Italy
[d] Department of Organic Chemistry, Instituto Regional de Investigación Científica Aplicada (IRICA), Universidad de Castilla-La Mancha, 13071, Ciudad Real, Spain
[e] Department of Organic Chemistry, Facultad de Ciencias y Tecnologías Químicas, Universidad de Castilla La Mancha, 13071, Ciudad Real, Spain
[f] Department of Chemical and Pharmaceutical Sciences, University of Trieste, 34127, Trieste, Italy
[g] Center for Cooperative Research in Biomaterials (CIC BiomaGUNE), Basque Research and Technology Alliance (BRTA), Paseo de Miramón 194, 20014, Donostia San Sebastián, Spain
[h] Basque Foundation for Science (IKERBASQUE), 48013, Bilbao, Spain

HIGHLIGHTS

- Environmentally relevant depositions of Graphene Oxide (GO) on flowers were applied.
- Neither pollen adhesion nor fruit formation were significantly affected.
- Seed development and germination were affected only at 22.1 ± 7.2 ng mm^{-2}
- The effects were caused by the residues of the production process still bound to GO.
- The first safety limits for a seed plant concerning "out-of-the-box" GO are given.

GRAPHICAL ABSTRACT

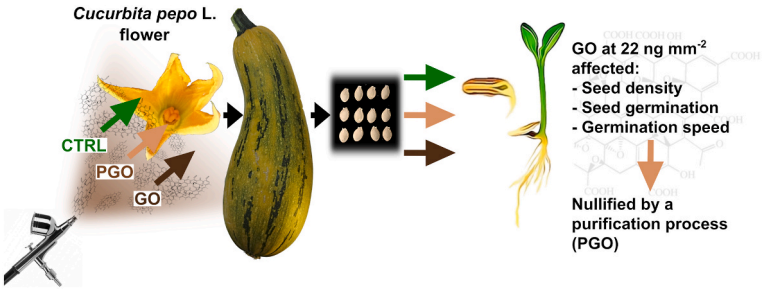

ARTICLE INFO

Handling Editor: Prof Willie Peijnenburg

Keywords:
Air pollution
Crops
Emerging pollutant
Flower biology
Nanoparticles
Production contaminants

ABSTRACT

The increasing use of graphene-related materials (GRMs) in everyday-life products raises concerns for their possible release into the environment and consequent impact on organisms. GRMs have widely varying effects on plants and, according to recent evidences, graphene oxide (GO) has the potential to interfere with the sexual reproduction owing to its acidic properties and production residues. Here, stigmas of the model plant *Cucurbita pepo* (summer squash) were subjected to simulated dry depositions of GO and GO purified from production residues (PGO). Stigmas were then hand-pollinated and GRM deposition was checked by ESEM and confocal microscopy. Analysis of stigma integrity, pH homeostasis and pollen-stigma interactions did not reveal negative effects. Fruit and seed production were not affected, but GO depositions of 22.1 ± 7.2 ng mm^{-2} affected the normal development of seeds, decreasing seed dimensions, seed germination and germination speed. The elemental analysis revealed that GO has significant quantities of production residues, such as strong acids and oxidants, while PGO has only traces, which justifies the differences observed in the effects caused by the two

* Corresponding author. via L. Giorgieri, 10, 34127, Trieste, Italy.
E-mail address: fcandotto@units.it (F. Candotto Carniel).

https://doi.org/10.1016/j.chemosphere.2022.137138
Received 2 September 2022; Received in revised form 1 November 2022; Accepted 2 November 2022
Available online 4 November 2022

materials. Our results show that GO depositions of up to 11.1 ± 3.6 ng mm^{-2}, which fall within the variation range of total dry particulate matter depositions reported in the literature, are safe for reproduction of *C. pepo*. This is the first "safety" limit ever recorded for depositions of "out-of-the-box" GO concerning the reproduction of a seed plant. If confirmed for wind-pollinated species, it might be considered for policymaking of GRMs emissions in the air.

1. Introduction

The first monolayer of graphene was isolated in 2004 (Novoselov et al., 2004), an event that kindled the research interest in graphene-related materials (GRMs) (Novoselov et al., 2012). GRMs have extraordinary chemical and physical properties that lead to innovative applications in many fields of technology (Bonaccorso et al., 2015; Joshi et al., 2018; Shamsaei et al., 2018). Many GRMs-enriched products, such as concrete, tires, asphalts and sports equipment, have already reached markets and civil society (Ron Mertens, 2021), and new ones will come soon. Indeed, the forecasted GRMs volume will be around 3800 t y^{-1} in 2026 (Ron Mertens, 2021), *i.e.*, orders of magnitude higher than the actual production of other carbon-based nanomaterials (NMs) (Ron Mertens, 2021).

GRM-enabled products will offer undeniable advantages, but they will wear out, break, and might be improperly disposed of at the end of their life cycle. This will cause an involuntarily GRMs release into the environment. A voluntary, direct release is also predictable if applications of GRM-composites as paints and protective coatings (Nine et al., 2015), pesticides (Liu et al., 2017; Wang et al., 2019), plant fertilizers (An et al., 2017; Andelkovic et al., 2018; Kabiri et al., 2017), sand improvers for soil remediation (Maliyekkal et al., 2013), and drug enhancers (Miraftab and Xiao, 2019) will reach the market. So far, despite GRMs nanoparticles have been recorded only in work places (Boccuni et al., 2020; Pingue et al., 2018), their emissions into the environment should be expected as already envisaged for other carbon-based NMs (Sun et al., 2014).

Two-dimensional (2D) GRMs nanoparticles are exceptionally lightweight. Once into the atmosphere, they could cover very long distances, as observed for fine and ultrafine carbon black (Qi and Wang, 2019), and then settle on soil, water bodies or vegetation with effects on the functionality of ecosystems that are still largely unknown.

To date, literature reports contradictory findings on the effects of GRMs on seed plants, probably because of different experimental conditions (concentration, exposure, materials, protocols, time etc.), plant developmental stages (seed, seedling, adult plants etc.), and/or species tested (Fadeel et al., 2018; Montagner et al., 2017). Leaves, stems, flowers and fruits normally intercept airborne particulate matter (PM) (Tretiach et al., 2011). This was also recently confirmed for airborne GRMs, which can be intercepted and retained by flowers of anemophilous plants (Zanelli et al., 2022). GRMs that settle on flowers might easily interfere with the fundamental process of sexual reproduction, because *in vitro* studies revealed that few-layer graphene (FLG) and graphene oxide (GO) decrease pollen germination and (limited to GO) pollen tube growth (Candotto Carniel et al., 2018, 2020). These effects were attributed to mechanical damage or to the oxygen functional groups of GO which can affect pH homeostasis and Ca^{2+} bioavailability (Candotto Carniel et al., 2018). Successive *in vivo* studies highlighted that FLG, GO, GO purified from production process residues (PGO), and muscovite mica, *i.e.* a naturally occurring 2D-NM, reduced pollen adhesion and germination on the stigma of the crop model plant *Cucurbita pepo* L. (summer squash), without injuring stigmas or pollen grains (Zanelli et al., 2020, 2021). However, when applied in massive amounts (1 mg per stigma), GO affected also fruit and seed development of *C. pepo* (Zanelli et al., 2021).

The abovementioned studies have shown that GO negatively affected various steps of the sexual reproduction process, both *in vitro* and *in vivo*, but in the latter case at quantities incompatible with realistic PM deposition processes. Moreover, it remains unclear what caused the heavy effects, and how.

Commercial GOs often contain residues from the production process as impurities depending on the method used to oxidize graphite, the most common being the Hummers' and its modified versions (Hummers and Offeman, 1958; Marcano et al., 2010; Ali-Boucetta et al., 2013; Barbolina et al., 2016). These impurities include potentially toxic elements (PTE), such as Cr, Fe and Mn, that as ions can be both coordinated to the oxygen functional groups of the GO lattice (Dziewięcka et al., 2016; Panich et al., 2012) and dissolved in the aqueous suspensions of GO (Sun et al., 2021). PTE ions in contact or internalized into cells might have an important role in the observed phytotoxicity (Barbolina et al., 2016; Zanelli et al., 2022) as they can impair the intracellular ROS balance (Anjum et al., 2015). A clear example is given by Ag ions: when bound to a nanoparticle or dissolved in the pollen germination medium, they cause a ROS overproduction or shortage, respectively, affecting the elongation of *Actinidia deliciosa* var. *deliciosa* (kiwifruit) pollen tube tips (Speranza et al., 2013).

Our working hypothesis is that at environmentally relevant quantities, the potential adverse effects of airborne GO could stem from the substances bound to the graphene lattice as residues of the production process, rather than from the intrinsic acidic properties of GO. To test this hypothesis, we exposed stigmas of *C. pepo* to simulated dry depositions of GO and PGO at realistic environmental concentrations, *i.e.* of the same order of magnitude of heavily PM polluted sites, thanks to the application of a new exposure method appropriately modified (Zanelli et al., 2022). *Cucurbita pepo* stigmas were then hand-pollinated, and fruit and seed production and development were assessed to estimate a "safety" limit for GO deposition, according to an approach that could be profitably extended to other plant species. The sexual reproduction of seed plants is indeed a pivotal process for most terrestrial ecosystems and crop production. Understanding whether plausible exposures to GO dry nanoparticles affect it, is essential to anticipate and promptly respond to possible negative scenarios that could occur if GRMs will become commonplace in our daily lives.

2. Materials and methods

2.1. GO preparation and characterization

Graphene oxide (GO; batch #GOB067) was kindly supplied by Graphenea (San Sebastián, Spain). The material was characterized as reported by Fusco et al. (2020).

For the experiments, GO was purified from the residues of the production process according to Ali-Boucetta et al. (2013). The supernatants removed after each purification step were saved and pooled (from here on referred to as GO-purification residue, $_{GO}$PR).

Quantitative elemental analyses were performed on 100 μg mL^{-1} GO, PGO and $_{GO}$PR dispersions by inductively coupled plasma mass spectrometry (ICP-MS) with a NexION 350X spectrometer (PerkinElmer, Waltham, MA, USA) in KED mode for Cd, Cr, Cu, K, Mn, Pb, and by inductively coupled plasma optical emission spectrometry (ICP-OES) with an Optima 8000 Spectrometer (PerkinElmer) for S. Approximately 4 mL of GO dispersions were filtered through a GHP Acrodisc (Pall Corporation, Port Washington, NY, USA) syringe filter (pore size: 0.22 μm) and then mixed with 50 μL of HNO_3 69% (Normatom, VWR, Milan, I), 0.5 mL (for a final concentration of 50 μg L^{-1}) of SC, Y, and Ho standard solutions used as internal standards (Sigma Aldrich, Milan, I),

and adjusted to a final volume of 5.0 mL with MilliQ water. The elemental concentration was then corrected on the basis of the relative dilution factor. The limits of detection (LOD) are listed in Table 1.

PGO and $_{GO}$PR flakes were observed with a JEM 2100 (JEOL Ltd., Tokyo, JP) high-resolution transmission electron microscope (HRTEM) to obtain their lateral dimension distributions. PGO and $_{GO}$PR dispersions were centrifuged at 4800×*g*, the supernatant and the precipitated fraction separated, then drop-casted on nickel grids (3.00 mm, 200 mesh), dried under vacuum, and observed at an accelerating voltage of 100 kV. Lateral dimension distributions were measured with FIJI software (NIH, Bethesda, MD, USA) (Schindelin et al., 2012).

2.2. Plant material

The squash marrow *Cucurbita pepo* L. ssp. *pepo "greyzini"* is an entomophilous, monoecious therophyte with short internodes and with indeterminate growth and reproduction (Nepi and Pacini, 1993; Winsor and Stephenson, 1995). Male flowers appear about two months after seed germination, 2–3 weeks before female ones; both flowers are produced throughout the remaining of the growing season. Each flower develops individually and lasts for only one day after anthesis (5–11 a.m.). Female flowers of *C. pepo* bear a single inferior ovary with one style and three stigmas, each made of two lobes (Winsor and Stephenson, 1995). Plants were cultivated from seeds [purchased from Salto di Fondi - Società Cooperativa Agricola (Fondi, I)] in greenhouse (c. 18–22 °C). Plants were irrigated daily at ground level, fertilized (Concime universale Asso di Fiori, Cifo, I) and treated every two weeks with antimycotics (Azupec 80WG, Ascenza Agro, Torres Vedra, P; Jupiter WG, Isagro Spa, Adria, I).

2.3. Experimental design

The effects of GO dry nanoparticles on sexual reproduction of *C. pepo* were investigated in two experiments. In a first experiment, morphometric analyses were performed on fruits developed from GOs-exposed female flowers of *C. pepo*, measuring their mass and dimensions, and assessing seed production. Subsequently, morphometric and performance analyses (germination percentage and speed, and seedling development) were performed on seeds collected from the aforementioned fruits. In a second experiment, the effects of GO and PGO on the stigmatic surface of *C. pepo* female flowers were assessed in terms of morphological integrity and pH homeostasis, as well as pollen adhesion and pollen germination on the stigma.

Table 1
Element content and relative limit of detection (LOD) of distilled water (dH_2O), suspensions of 100 μg mL^{-1} graphene oxide (GO), purified GO (PGO) and GO production residues ($_{GO}$PR); for the latter, the values refer to the analysis of the pooled aliquots deriving from the purification procedure (for more details, see section 2.1). Data are reported as mean ± standard deviation. n = 3–5.

Element	LOD μg L^{-1}	dH_2O	GO	PGO	$_{GO}$PR
Cd	0.001	< LOD	< LOD	< LOD	0.05 ± 0.05
Cr	0.008	0.02 ± 0.01	0.05 ± 0.02	0.02 ± 0.00	0.35 ± 0.07
Cu	0.003	0.42 ± 0.10	0.29 ± 0.14	0.38 ± 0.09	3.83 ± 2.35
K	0.002	4.89 ± 1.46	329 ± 29.1	21.3 ± 2.57	2968 ± 2434
Mn	0.001	0.03 ± 0.01	593 ± 783	12.0 ± 8.44	4278 ± 334
Pb	0.002	0.05 ± 0.01	0.07 ± 0.02	0.08 ± 0.05	0.26 ± 0.18
S	250	< LOD	9167 ± 798	594 ± 190	49,208 ± 3254

2.4. Exposure of stigmas to GO materials

Receptive stigmatic surfaces of *C. pepo* were treated simulating dry depositions of airborne GO or PGO using the method proposed by Zanelli et al. (2022), suitably modified to obtain controlled and quantifiable depositions. The latter were obtained by nebulizing 5 mL of 90% v/v ethanol/water solutions enriched with GO (0, 25, 50 or 100 μg mL^{-1}) or PGO (100 μg mL^{-1}) with an airbrush (AWSUC, Shenzhen Deshunke Technology Co., Ltd, Longgang, PRC: nozzle diameter: 0.3 mm; applied pressure: 1.4 Bar; estimated flow rate 23–25 L min^{-1}) directly onto stigmatic surfaces. Preliminary tests were conducted to find the correct distance between the airbrush and the sample which allowed the complete liquid-gas phase transition of the nebulized ethanol/water solution before reaching the stigmatic surface. At 21 °C (room temperature), this condition was achieved by placing the airbrush tip 30 cm from the stigma and then activating the airbrush. No damage was observed in control stigmas treated with the ethanol/water solution. A specific protocol was developed to estimate the depositions obtained with different GO dispersions (see SI: S1, S2, Figs. S1 and S2 and Table S1). Under these conditions, the nebulization of 0, 25, 50 and 100 μg mL^{-1} dispersions corresponded to dry depositions of 0, 5.5 ± 1.8, 11.1 ± 3.6 and 22.1 ± 7.2 ng mm^{-2}, respectively (hereafter referred to as CTRL, GO5.5, GO11 and GO22 or PGO22). These deposition levels were selected on the basis of inventories on depositions of total PM available for rural, urban and industrial areas of China (min.: 27 ng mm^{-2} d^{-1}; max.: 110 ng mm^{-2} d^{-1}; Pan and Wang, 2015) and the United States (min.: 3.5 ng mm^{-2} d^{-1}; max.: 27 ng mm^{-2} d^{-1}; Oldani et al., 2017) and inventories on total daily dry depositions of K and SO_4 provided by USEPA (min.: 0.027 ng mm^{-2} d^{-1}, max.: >0.27 ng mm^{-2} d^{-1}, for both: www.epa.gov/castnet).

2.5. Fruit and seed biometrics

To test the effect of GO on fruit and seed production, all three stigmas of one female flower per plant (n = 11–17) were treated with GO and PGO as described in section 2.4. After 3 h, treated flowers were hand-pollinated with a brush to ensure even distribution of pollen all across three stigmatic lobes. For this purpose, pollen was harvested from *C. pepo* male flowers ~2:30 h after flower blossoming (~7:30 a.m.) and its viability assessed by the fluorescein diacetate (Sigma-Aldrich, Munich, DE) fluorochromatic reaction, counting at least 200 pollens (Heslop-Harrison and Heslop-Harrison, 1970). Only pollen aliquots with viability higher than 70% were used.

Fruits developed from treated stigmas (hereafter referred to as CTRL, GO5.5, GO11, GO22 and PGO22 fruits) were harvested five weeks after pollination. Fresh mass, length, and maximum circumference of fruits were measured. Fruits were kept under laboratory conditions (21 °C and dim light) for further 9 weeks to allow complete seed ripening. Seeds were then collected, rinsed in dH_2O to remove residual pulp, dried for 24 h and then counted. Seeds (hereafter referred to as CTRL, GO5.5, GO11, GO22 and PGO22 seeds) were further dehydrated, first for one week under laboratory conditions, then for one month over silica gel (air RH ~ 3%). The dry mass of each seed was measured gravimetrically, then the seeds were photographed on a black cloth, and the digital images were analysed with software FIJI to calculate the projected area (seed area). Seed density was calculated as the mass/area ratio.

2.6. Seed and seedling performance

The effect of GO was checked on the germination of seeds developed from GO and PGO-treated flowers and on seedlings germinated from these seeds. Seeds were sampled using a stratified random strategy based on seed biometric characterization. Strata were defined on the basis of the quartiles of the distribution of seed mass values. Twenty-eight seeds, seven per stratum, were sampled from CTRL, GO22 and PGO22 samples.

Seeds were rehydrated overnight in tap water at RT, surface

sterilized with a 1% NaClO water solution for 5 min and then rinsed in dH_2O for 3 min (Souza et al., 2013). Seeds were then placed over wet absorbent paper (5.07 ± 0.76 mL of H_2Od) in Parafilm sealed Petri dishes (12.5 cm diam.) (Rajjou et al., 2011) and incubated in the dark in a MIR-153 incubator (Sanyo Electric. Co. Ltd., Osaka, JP) at 25 °C.

2.6.1. Seed germination and seedling biometrics

Seed germination was checked daily and germination rate was assessed on the fourth day after sowing and expressed as percentage of total seeds sown (Souza et al., 2013). Seeds were considered germinated when the rootlet was at least 5 mm long (Souza et al., 2013). Speed of germination was estimated for six days after sowing by calculating the germination speed index (GSI) proposed by Maguire (1962) and modified by Ranal and de Santana (2006). Not germinated seeds were opened and examined to check the developmental status of embryo and cotyledons. Seedlings were photographed six days after sowing and the captured digital images were analysed using FIJI software to measure the seedling length (shoot + root). Germinated seeds were oven dried at 60 °C for 48 h (Siddiqui et al., 2014), and kept over silica gel (air RH ~ 3%) for two days before measuring the seedlings dry mass.

2.7. GO and PGO effects on stigmatic surfaces and pollen-stigma interactions

The effect of GO and PGO nanoparticles on the stigmatic surface and the pollen-stigma interactions were tested on individual stigmas: one stigma per flower (n = 3–6) was treated as CTRL, one as GO22 and one as PGO22, as described in section 2.4. The stigmas were treated individually by placing a piece of aluminium foil between the treated stigma and the other two, and then kept under laboratory conditions (see above) for 3 h. Differently, the effect of GO and PGO acidity on the stigma pH homeostasis was tested using all the stigmatic surfaces of single flowers.

2.7.1. GO and PGO effects on the stigmatic surface

Three CTRL, GO22 and PGO22 stigmas were excised, mounted on aluminium stubs, and observed using a Quanta250 SEM (FEI, Oregon, USA) in environmental mode (ESEM) (details in Zanelli et al., 2022). The entire stigmatic surface of each sample was examined and 10 to 15 micrographs were taken per sample. Micrographs were then carefully analysed to detect structural modifications to the stigmatic surface such as papillae agglutination and/or shrinkage, and release of cytoplasm as a result of GOs presence.

2.7.2. Effects of GO and PGO acidity on the stigma pH homeostasis

Pristine stigmas were soaked in 10 mL $NaNO_3$ 0.01 M solutions enriched with GO to concentrations of 0, 25, 50 or 100 μg mL^{-1} or with PGO to 100 μg mL^{-1}. The pH was recorded after stabilization, *i.e.*, 45 min after stigma soaking (n = 6), using a HI5521 pH-meter with HI1131B electrode (Hanna Instruments Italia S.r.l., Padua, I), following Zanelli et al. (2021). Care was taken to soak only the stigmatic surface (all three stigmas) avoiding possible injuries from sample manipulation. Stigmas of similar size were selected: their surface areas ranged from 622 to 1026 mm^2 (*i.e.*, 3 times the mean stigmatic surface ± 3 times the standard deviation of a mean stigma, see SI). For comparison, pH was also recorded in dH_2O and $NaNO_3$ 0.01 M solutions enriched with GO to concentrations of 0, 25, 50 or 100 μg mL^{-1} or with PGO to 100 μg mL^{-1}, without soaking any stigmatic surface ("blanks").

2.7.3. Pollen adhesion and germination on the stigmatic surface

CTRL, GO22 and PGO22 stigmas (n = 6) were hand-pollinated with 3 ± 0.5 mg of pollen (corresponding to c. 2400 ± 500 pollen grains) using a brush. Pollen was gently and homogeneously brushed on a 4 × 4 mm surface using a greaseproof, paper frame. The pollen was then allowed to germinate for 40 min under laboratory conditions (see above). Pollen adhesion and germination on the stigma were assessed as described in Zanelli et al. (2020). Germination rate was calculated as the percentage of germinated pollen still adhering to the stigma (n = 6) by checking 221 ± 31 pollen grains per stigma.

2.8. Statistical analysis

Statistical analysis was performed using the Dplyr software package in the R environment (R, version 3.6.3., The R foundation for statistical analysis) (Bunn, 2008). Significant differences for the selected biometric parameters of fruits and seeds were assessed with generalized linear models (GLMs), assuming treatments (*i.e.*, the amounts of GO and PGO dry depositions) as categorical predictors. The same approach was used to test for significant differences in pollen adhesion and germination rate on the stigma. Differences among treatments were determined using the post-hoc pairwise *t*-test, using the Bonferroni correction method. When the distribution of GLM residuals was not normal, differences among experimental groups were tested with the Kruskal-Wallis nonparametric ANOVA followed by pairwise Wilcoxon-Mann-Whitney test as *post-hoc* test. Differences with Pr- and *p*-values < 0.05 were considered statistically significant.

3. Results

3.1. GO, PGO and $_{GO}$PR characterization

Elemental analysis revealed that GO consisted of 59.4 ± 0.1% C, 36.6 ± 0.1% O, 2.5 ± 0.1% S, 1.4 ± 0.1% H, 0.1 ± 0.1% N. The Raman spectra of GO had the two characteristic D and G bands, whose maxima were ~1350 and ~1600 cm^{-1}, respectively (SI, Fig. S3A). GO flakes had lateral dimensions ranging from 0.5 to 30 μm, with an average of 15.1 ± 0.4 μm and an average thickness of six layers measured by XRD (Fusco et al., 2020). Representative HR-TEM and ESEM images are reported in SI (Figs. S3B–D).

In GO and PGO dispersions, the mean content of Cd and Cr was below the detection limit (LOD); the content of K, Mn and S ranged from ~10 to ~ 10,000 μg L^{-1} and was on average an order of magnitude higher in GO dispersions than in PGO ones (Table 1). Only the Cu and Pb contents were lower in GO dispersions than in PGO ones, although quite similar: ~0.3 and ~0.07 μg L^{-1} for Cu and Pb, respectively. The elemental content of $_{GO}$PR dispersions was always one or two orders of magnitude higher than that of GO and PGO.

HRTEM analysis showed that a small fraction of flakes remained in the $_{GO}$PR dispersions after the purification process (Fig. S3F). In both the $_{GO}$PR and PGO dispersions, at least the 30% of flakes had a lateral dimension greater than 7 μm (Figs. S3E and F). In $_{GO}$PR dispersions more than 50% of flakes had lateral dimensions in the range 0.5–2.0 μm, whereas in PGO dispersions only c. 14% of flakes were smaller than 2.0 μm. Purification of GO removed c. 1.8–5.4% of the flakes smaller than 0.5 μm (Figs. S3E and F).

3.2. Fruit and seed development from GO- and PGO-treated stigmas

Fruits from CTRL and treated, fertilized pistils ripened normally. They had similar fresh mass, length and circumference, and produced similar numbers of seeds (Fig. S4, Table S2). Mean seed mass did not differ among CTRL (165.1 ± 43.1 mg), GO5.5, GO11 and PGO22 seeds, whereas it was significantly lower by 21% in GO22 seeds compared with CTRL (Fig. 1A, Table S3). Conversely, seed area differed significantly among treatments: it was the 12% and 7% lower in GO5.5 and GO11 seeds, respectively, than in CTRL seeds and 3% higher in GO22 seeds (Fig. 1B and Table S3).

The seed area of PGO22 was not different from that of CTRL. Accordingly, seed density had an opposite trend: it was significantly higher in GO5.5 and GO11 seeds than in CTRL seeds by 12% and 19%, respectively, and lower in GO22 seeds by 19% (Fig. 1C and Table S3). The density of PGO22 seeds was not different from that of CTRL seeds. In

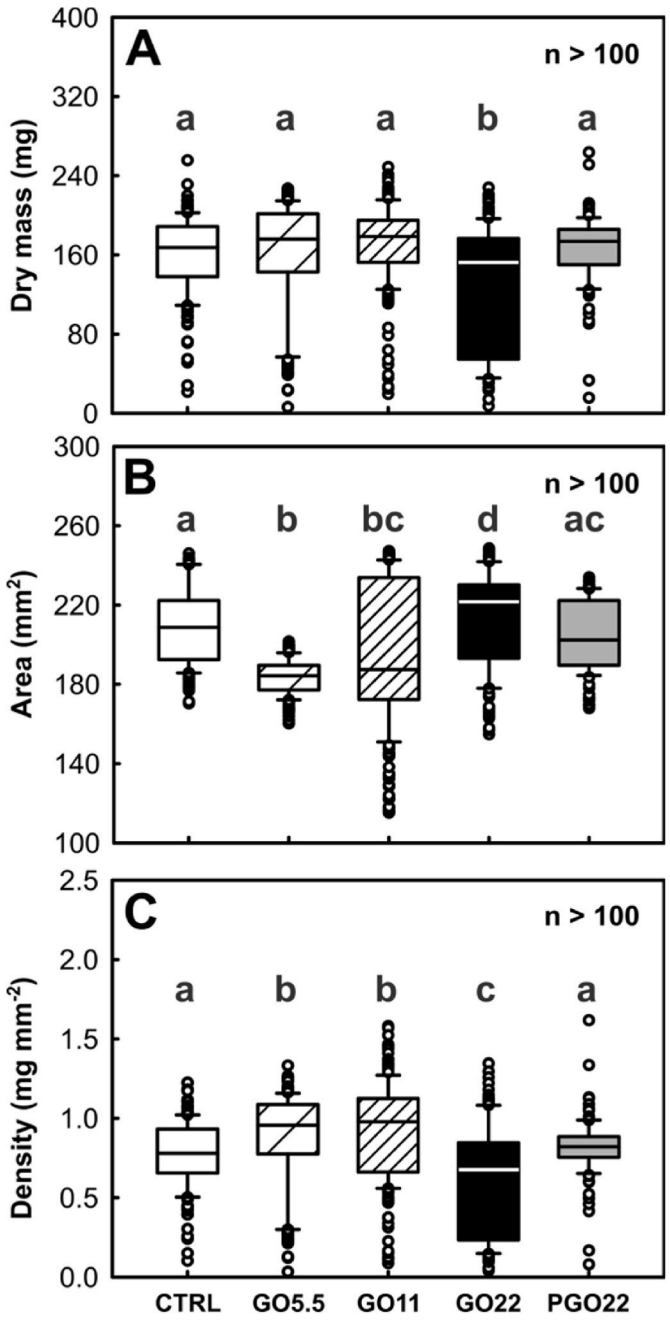

Fig. 1. Morphometric characterization of *Cucurbita pepo* seeds developed from flowers treated with dry depositions of 0, 5.5, 11 or 22 μg mm^{-2} of graphene oxide (GO) (CTRL, GO5.5, GO11 and GO22, respectively) or 22 μg mm^{-2} of purified GO (PGO22) and hand-pollinated after 3 h (for more details, see sections 2.4, 2.5): dry mass (A); area of one face of the planar seeds (B); density (C) calculated as the ratio between dry mass and area of each single seed. Boxplots represent the median second and third quartiles, whereas whiskers include non-outlier range (calculated as ± 3 s.d.). Statistically different groups are marked with different letters (non-parametric ANOVA of Kruskal-Wallis and Wilcoxon-Mann-Whitney *post-hoc* test; see Tables S4 and S5).

summary, only GO deposition of 22 ng mm^{-2} had a negative effect on all seed biometric parameters, whereas the same PGO deposition had no effect (Fig. 1, Table S3).

3.3. Performance of GO and PGO seeds and seedlings

CTRL seeds had a germination of 86 ± 3%, similar to that of PGO22 seeds (Fig. 2A, Table S4), while GO22 seeds germination decreased significantly by 31% (Fig. 2A, Table S4). GO22 seeds also had a significantly lower GSI (- 37%) than CTRL seeds, and again, PGO22 seeds had a GSI not different from CTRL seeds (Fig. 2A, Table S4). The examination of non-germinated seeds from CTRL revealed different developmental states of the embryo and cotyledons: (*i*) embryo axon present, cotyledons normally developed (Fig. S5A); (*ii*) embryo axon present, cotyledons only partially developed (Fig. S5B); (*iii*) embryo axon present, cotyledons not recognizable (Fig. S5C); (*iv*) embryo and cotyledons not recognizable (See Fig. S5D).

For GO22 seeds, the number of seeds in categories (*i*) and (*ii*) was 9% and 10% lower, respectively, compared with CTRL seeds, while the number of seeds in categories (*iii*) and (*iv*) was 7% and 12% higher, respectively (Table S5).

Seedlings developed from CTRL, GO22 and PGO22 seeds had similar length (shoot + root) and dry mass (Fig. 2B, Table S4).

3.4. GO and PGO effect on morphology and pH homeostasis of the stigmatic surface, and in vivo pollen stigma-interactions

The stigmatic surface of *C. pepo* consists of stigmatic papillae, *i.e.* clusters of finger-like cells receptive to pollen (Fig. 3A and B). ESEM observations revealed that a GO deposition of 22 ng mm^{-2} did not affect the integrity of the stigmatic surface as the treated samples did not show wilted cells or cytoplasmic leachates and the papillae maintained their original shape (Fig. 3B vs. C, D) even though GO flakes were clearly visible on the stigmatic surface (Fig. 3C and D).

The pH of 25, 50 and 100 μg mL^{-1} GO dispersions in dH_2O was 3.9 ±

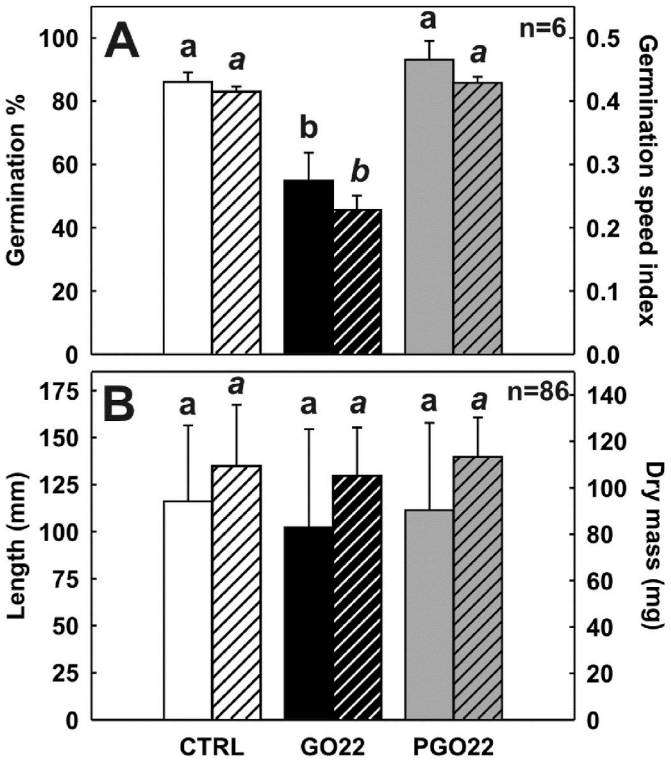

Fig. 2. Performance of *Cucurbita pepo* seeds (A) and seedlings (B), developed from flowers treated with dry depositions of 0 (CTRL), 22 μg mm^{-2} of graphene oxide (GO22) or purified GO (PGO22) and hand-pollinated after 3 h (for more details, see sections 2.4, 2.6): germination percentage (full bars) and germination speed index (patterned bars) (A), and shoot + root length (full bars) and dry mass (patterned bars) (B). Values are means ± s.d. Statistically different groups are marked with different letters (non-parametric ANOVA of Kruskal-Wallis followed by Wilcoxon-Mann-Whitney *post-hoc* test; see Tables S4 and S5).

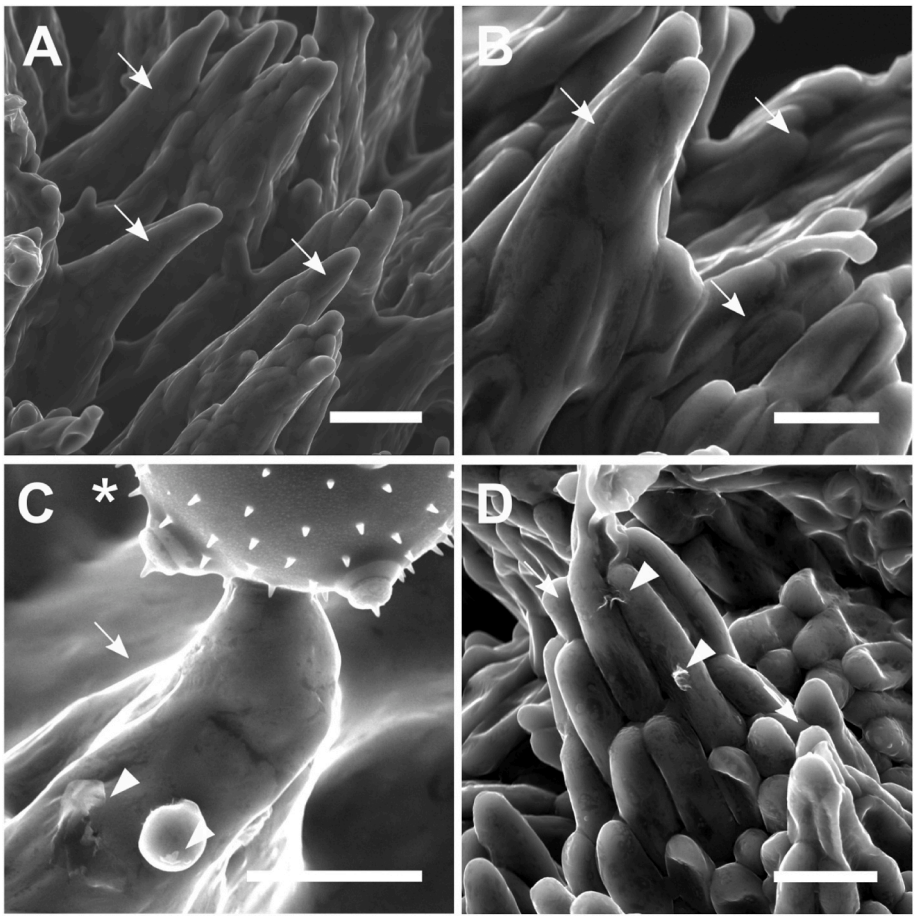

Fig. 3. ESEM micrographs of stigmas of *Cucurbita pepo* flowers treated with dry depositions of 0 (CTRL) (A, B) or 22 μg mm^{-2} of graphene oxide (GO) (C) or purified GO (D) and pollinated after 3 h (for more details, see sections 2.4, 2.7). Stigmatic papillae, GOs flakes/nanoparticles and pollen grain are indicated with arrows, arrowheads and asterisk, respectively. Bars = 100 μm.

0.1, 3.6 ± 0.1 and 3.3 ± 0.1, respectively. For 100 μg mL^{-1} PGO dispersions the pH was 5.8 ± 0.3. $NaNO_3$ solutions without GO had a circumneutral pH (Table S6), which decreased with increasing concentration of GO, and reached a value of 3.3 ± 0.1 in 100 μg mL^{-1} GO dispersions. At the same concentration of PGO, the pH was 4.6 ± 0.1. When stigmatic surfaces were immersed in $NaNO_3$ solutions without GOs, the pH stabilized at 6.5 ± 0.1 (Table S6). Subsequent addition of GO aliquots gradually lowered pH, to a minimum of 5.6 ± 0.3 at a concentration of 100 μg mL^{-1}. Addition of PGO at the same concentration also lowered pH, but to a minimum of 6.2 ± 0.1 (Table S6).

Pollen adhesion and germination on CTRL, GO22 and PGO22 stigmas did not differ among treatments (Fig. 4 and S6, Table S7).

4. Discussion

Over the past fifty years, it was demonstrated that airborne pollutants, ranging from gaseous oxides (e.g., SO_x) (Cox, 1984) to solid PM (Farmer, 1993; Zhang et al., 2019), can be a dangerous threat to the sexual reproduction of seed plants. These substances can affect the reproduction process both through their physical interaction with reproductive organs (Waser et al., 2017; Zanelli et al., 2020; Zhang et al., 2019), and by chemically altering the fine-tuned processes of pollen tube germination and elongation (Cox, 1984; Du Bay and Murdy, 1983; Hughes and Cox, 1994). Xenobiotics such as fungicides, pesticides, herbicides and metal nanoparticles can also have similar consequences and eventually alter fruit and/or seed production (Bristow, 1981; Cox, 1988; Wetzstein, 1990; Speranza et al., 2010, 2013; Gillespie et al., 2014).

GRMs have all the characteristics of emerging pollutants, as they will be intensively produced and used (Ron Mertens, 2021), will be easily dispersed in the air thanks to their 2D geometry and lightness, and can affect organisms (Montagner et al., 2017). In addition, the recent discovery that the stigmas of anemophilous plants can intercept and retain airborne GO even at a very low air concentration (Zanelli et al., 2022), reinforces the concerns about the unintentional release of GRMs into the environment. For these reasons, *C. pepo* stigmas were treated here with simulated dry depositions of GRMs at levels which fall within the variation range of total dry PM depositions reported in the literature. Fruit and seed production was never affected by GO or PGO depositions (Fig. S4), even at the highest levels used in this work (22.1 ± 7.2 ng mm^{-2}).

However, depositions of 22 ng mm^{-2} of GO negatively affected seed development decreasing seed density, germination and germination speed (Figs. 1B and 2A). The decrease in germination was due to the higher percentage of abortive seeds, *i.e.*, lacking a properly formed embryo axon and cotyledons. Impaired seed development without detectable fruit alterations has been previously observed in plants exposed to other xenobiotics (Heazlewood et al., 2005; Saladin and Clement, 2005; Gillespie et al., 2014; Bodnar et al., 2019). This could be due to a decreased pollen load on the stigmatic surface, resulting in a lower density of pollen tubes growing through the stigma and, consequently, lower competition along the transmitting tract of the style (Ter-Avanesian, 1978; Winsor et al., 1987; Hiscock and Allen, 2008). The presence of xenobiotics onto the stigma could actually cause this effect by: (*i*) damage to the receptive surface, (*ii*) inadequate pollen adhesion; (*iii*) impaired pollen germination and pollen tube elongation.

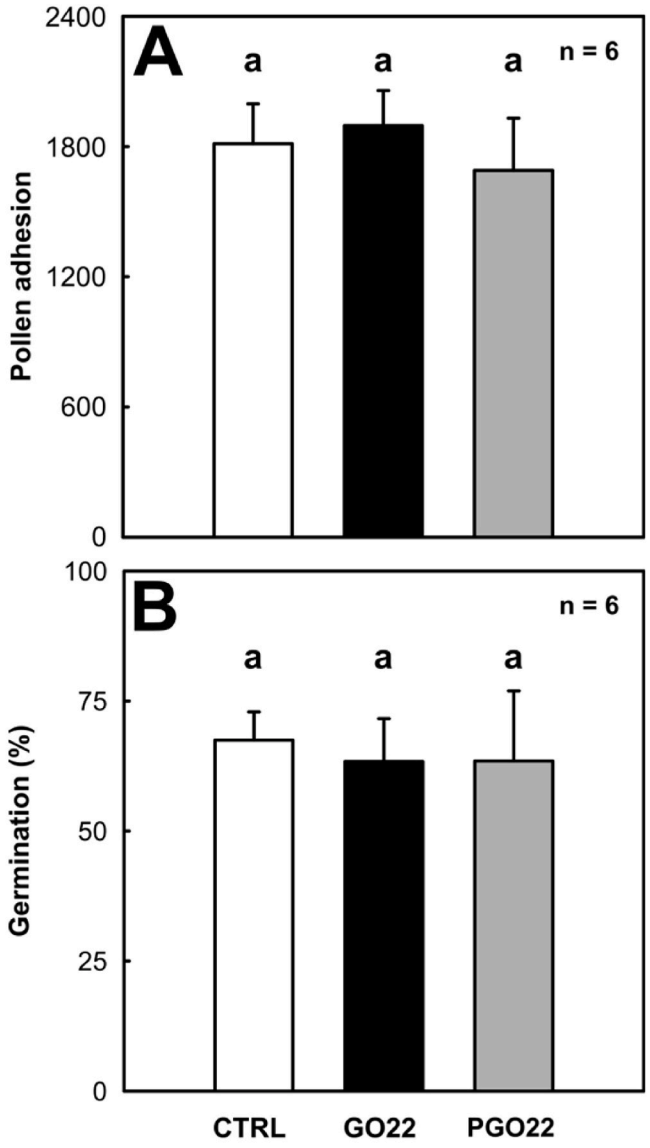

Fig. 4. Pollen-stigma interaction of *Cucurbita pepo* flowers treated with dry depositions of 0 (CTRL), 22 μg mm^{-2} of graphene oxide (GO22) or purified GO (PGO22) and hand-pollinated after 3 h (for more details, see sections 2.4, 2.7): pollen adhesion (A) and germination over CTRL-, GO100- and PGO-treated stigmas (B). Values are means ± s.d (n = 6). Statistically different groups are marked with different letters (non-parametric ANOVA of Kruskal-Wallis followed by Wilcoxon-Mann-Whitney *post-hoc* test; see Tables S4 and S5).

However, in this study GOs deposition did not cause any of the above effects (Figs. 3 and 4, S6), despite the evident presence of GOs flakes adhering to the stigmatic surface (Fig. 3C and D). This, together with the increased percentage of non-germinating, abortive seeds supports the hypothesis that GO at the highest dose affected the generative cell inside the developing pollen tube, that forms the gametes that fertilize the egg cell and the polar nuclei in the embryo sac. *In vitro*, GO is toxic to pollen tube elongation mainly because of its acidic properties (Candotto Carniel et al., 2018), but also for possible physical damage and/or the presence of toxic impurities (Barbolina et al., 2016). In *C. pepo*, the negative effect of GO acidity can be excluded, since the stigmatic surface of this species has a remarkable pH stability – not documented before. Stigmas soaked in GO or PGO dispersions, increased pH of c. 2.5 units, from 3.29 to >5.6 (Table S6), a safe value for the pollen-stigma system of most species (Cox, 1983), including *C. pepo* (Nepi and Pacini, 1993).

The deposition of PGO over the stigma surface did not cause the negative effects of GO mentioned above when administered at the same surface density (*i.e.* 22.1 ± 7.2 ng mm^{-2}). This suggests that the negative effects might be due to the GO-production residues more than from GO itself. GO impurities have been thoroughly characterized from a chemical point of view (Panich et al., 2012, 2013; Pumera et al., 2012). Unfortunately, their effects were assessed only seldom in GO ecotoxicity tests, as evidenced by literature reviews (Montagner et al., 2017; Fadeel et al., 2018) and a further survey of the relevant literature (see Table S8). Also manufacturer's websites rarely report analyses underlying the presence of biological and chemical contaminants (Table S8). Therefore they were rarely considered when interpreting results (Petersen et al., 2014). Impurities originate directly from oxidizing reagents (e.g. $KMnO_4$) and strong acids (e.g. H_2SO_4) used in the production process, the most frequent being Hummers' (Hummers and Offeman, 1958) and modified Hummers' (Ali-Boucetta et al., 2013; Marcano et al., 2010) methods. Other impurities are likely introduced unintentionally as reagent contaminants (e.g. Cu, Cd, Ni, Pb, Zn etc.), usually in the range of 0.1–2.0 ppm, more in exceptional cases (Table S8). These impurities remain partially bound to the material and partially free in the GO dispersion. Some of them, such as Cd, Cr and Mn, are known to exert phytotoxic effects (Nagajyoti et al., 2010). Therefore, in order to attribute possible adverse effects exclusively to GO, purification procedures are required, but rarely performed (Ali-Boucetta et al., 2013; Candotto Carniel et al., 2018; Fadeel et al., 2018). The purification applied in this study greatly reduced the amount of K, Mn and S residues from GO, leaving only traces in PGO (Table 1). The lack of adverse effects observed in PGO treated flowers strongly supports our original hypothesis that the potential adverse effects of airborne GO stem from the residues of the production process, rather than from the intrinsic acidic properties of GO. Manganese should be identified as the major PTE, as it was particularly abundant in the GO suspensions used for treatments (593 ± 78 μg L^{-1}). Furthermore, it was recently reconfirmed that Mn can affect pollen germination and elongation of the pollen tube, as well as on other plant functions (Anjum et al., 2015; Li et al., 2019; Millaleo et al., 2010), at relatively low concentrations (≥0.549 μg L^{-1}) (Sawidis and Reiss, 1995; Sawidis et al., 2021).

Purification of GO also removed a small fraction of flakes, including the smallest ones (Figs. S3E and F). Notoriously, GO flakes with lateral dimension of less than 500 nm are those mainly responsible for the toxicity of the material, as they can penetrate or be internalized by cells (Ou et al., 2016). However, in our case only c. 1.8–5.4% of this fraction was removed by the GO purification (Figs. S3E and F). Moreover, TEM images of growing pollen tubes in contact with GO, in higher amounts and with smaller dimensions (~500 nm for GO, with 54% of the flakes <500 nm) (Candotto Carniel et al., 2020) than those tested here, showed no internalization of flakes. For the aforementioned reasons, we believe that the amount of potentially phytotoxic substances present as impurities in the GO batch is the most plausible cause of the observed effects.

Summarizing, depositions of GO up to 11.1 ± 3.6 ng mm^{-2} (GO11 treatment) are safe for *C. pepo* reproduction. However, further studies are needed to understand whether and at what deposition levels of GO, as well as other 2D-nanomaterials, might affect the sexual reproduction of other seed plants, and particularly wind-pollinated species, whose members include important crops (e.g., cereals such as barley, corn, rice or wheat) but also form the backbone of entire ecosystems (e.g., grasses or trees such as conifers or oaks).

5. Conclusions

In this study, we tested the effect of simulated GO dry depositions on the reproduction process of the crop and model plant *C. pepo*. GO and PGO neither compromised fruit production and development nor seed production. Pollen-stigma interactions were also not affected. Only the highest GO deposition tested, *i.e.* 22.1 ± 7.2 ng mm^{-2}, affected seed development and, consequently, seed germination and germination speed. The results on PGO strongly supports the hypothesis that the

impairment of seed development could be caused by GO impurities, rather than by GO itself, with Mn (from the production method) being the main suspect.

Finally, depositions of GO up to 11.1 ± 3.6 ng mm^{-2} are safe for the reproduction of *C. pepo*, and are in a relevant and comparable range with values reported in the literature for total and dry depositions. The threshold determined here is the first "safety" benchmark threshold for "out-of-the-box" GO depositions for the reproduction of seed plants ever reported: if also confirmed for wind-pollinated plants, such as grasses and conifers, this threshold might be considered for policy-making regarding airborne GRMs.

Credit author statement

Conceptualization: DZ, FCC, MT; Data curation: DZ; Formal Analysis: DZ; Funding acquisition: EV, MP, MT; Investigation: DZ, LF, EP, VJG; Methodology: DZ, FCC, LF, MT; Project administration: FCC, MT; Resources: DZ, FCC, MT; Supervision: FCC, MT; Validation: FCC, MT, EV; Visualization: DZ; Writing – original draft: DZ, FCC, MT; Writing – review & editing: FCC, MT.

Declaration of competing interest

The authors declare that they have no known competing financial interests or personal relationships that could have appeared to influence the work reported in this paper.

Data availability

Data will be made available on request.

Acknowledgements

This paper is dedicated to the memory of Prof. Ettore Pacini (University of Siena) for his outstanding contribution to the study of floral biology.

This work was supported by the Graphene Flagship Core 2 and Core 3 grant agreements (nr. 785219 and 881603, respectively) and The University of Trieste DOTTAMBIENTEVITA34-18. Part of this work was performed under the Maria de Maeztu Units of Excellence Program, Spanish State Research Agency – Grant nr. MDM-2017-0720. M. Prato is a recipient of the Carbon Bionanotechnology AXA Chair (2016–2023). The authors thank Andrea Pannozzo, and Ivana Tranquillini (Salto di Fondi - Società Cooperativa Agricola) for plants growth and fruit harvesting, Matteo Crosera (University of Trieste) for GOs elemental analysis, Davide Porrelli and Gianluca Turco (University of Trieste), for ESEM analysis.

Appendix A. Supplementary data

Supplementary data to this article can be found online at https://doi.org/10.1016/j.chemosphere.2022.137138.

Websites

www.us.epa.gov/castnet accessed the August 20, 2022.

References

Ali-Boucetta, H., Bitounis, D., Raveendran-Nair, R., Servant, A., Van den Bossche, J., Kostarelos, K., 2013. Purified graphene oxide dispersions lack *in vitro* cytotoxicity and *in vivo* pathogenicity. Adv. Healthc. Mater. 2, 433–441. https://doi.org/10.1002/adhm.201200248.

An, D., Liu, B., Yang, L., Wang, T.J., Kan, C., 2017. Fabrication of graphene oxide/polymer latex composite film coated on KNO_3 fertilizer to extend its release duration. Chem. Eng. J. 311, 318–325. https://doi.org/10.1016/j.cej.2016.11.109.

Andelkovic, I.B., Kabiri, S., Tavakkoli, E., Kirby, J.K., McLaughlin, M.J., Losic, D., 2018. Graphene oxide-Fe(III) composite containing phosphate – a novel slow release fertilizer for improved agriculture management. J. Clean. Prod. 185, 97–104. https://doi.org/10.1016/j.jclepro.2018.03.050.

Anjum, N.A., Singh, H.P., Khan, M.I.R., Masood, A., Per, T.S., Negi, A., Batish, D.R., Khan, N.A., Duarte, A.C., Pereira, E., Ahmad, I., 2015. Too much is bad—an appraisal of phytotoxicity of elevated plant-beneficial heavy metal ions. Environ. Sci. Pollut. Res. 22, 3361–3382. https://doi.org/10.1007/s11356-014-3849-9.

Barbolina, I., Woods, C.R., Lozano, N., Kostarelos, K., Novoselov, K.S., Roberts, I.S., 2016. Purity of graphene oxide determines its antibacterial activity. 2D Mater. 3 https://doi.org/10.1088/2053-1583/3/2/025025.

Boccuni, F., Ferrante, R., Tombolini, F., Natale, C., Gordiani, A., Sabella, S., Iavicoli, S., 2020. Occupational exposure to graphene and silica nanoparticles. Part I: workplace measurements and samplings. Nanotoxicology 14, 1280–1300. https://doi.org/10.1080/17435390.2020.1834634.

Bodnar, V.R., Lofton, J., Manuchehri, M.R., Zander, A.D., 2019. Impact of late-season herbicide applications on winter canola yield and seed quality. Agrosyst. Geosci. Env. 2, 180053 https://doi.org/10.2134/age2018.10.0053.

Bonaccorso, F., Colombo, L., Yu, G., Stoller, M., Tozzini, V., Ferrari, A.C., Ruoff, R.S., Pellegrini, V., 2015. Graphene, related two-dimensional crystals, and hybrid systems for energy conversion and storage. Science 347, 1246501. https://doi.org/10.1126/science.1246501.

Bristow, P.R., 1981. Effect of triforine on pollen germination and fruit set in highbush blueberry. Plant Dis. 65, 350–353. https://doi.org/10.1094/PD-65-350.

Bunn, A.G., 2008. A dendrochronology program library in R (dplR). Dendrochronologia 26, 115–124. https://doi.org/10.1016/j.dendro.2008.01.002.

Candotto Carniel, F., Gorelli, D., Flahaut, E., Fortuna, L., Del Casino, C., Cai, G., Nepi, M., Prato, M., Tretiach, M., 2018. Graphene oxide impairs the pollen performance of *Nicotiana tabacum* and *Corylus avellana* suggesting potential negative effects on the sexual reproduction of seed plants. Environ. Sci. Nano 5, 1608–1617. https://doi.org/10.1039/c8en00052b.

Candotto Carniel, F., Fortuna, L., Nepi, M., Cai, G., Del Casino, C., Adami, G., Bramini, M., Bosi, S., Flahaut, E., Martín, C., Vázquez, E., Prato, M., Tretiach, M., 2020. Beyond graphene oxide acidity: novel insights into graphene related materials effects on the sexual reproduction of seed plants. J. Hazard Mater. 393, 122380 https://doi.org/10.1016/j.jhazmat.2020.122380.

Cox, R.M., 1983. Sensitivity of forest plant reproduction to long range transported air pollutants: *in-vitro* sensitivity of pollen to simulated acid rain. New Phytol. 95, 269–276. https://doi.org/10.1111/j.1469-8137.1983.tb03493.x.

Cox, R.M., 1984. Sensitivity of forest plant reproduction to long range transported air pollutants: *in vitro* and *in vivo* sensitivity of *Oenothera parviflora* L. pollen to simulated acid rain. New Phytol. 97, 63–70. https://doi.org/10.1111/j.1469-8137.1984.tb04109.x.

Cox, R.M., 1988. Sensitivity of forest plant reproduction to long-range transported air pollutants: the effects of wet deposited acidity and copper on reproduction of *Populus tremuloides*. New Phytol. 110, 33–38. https://doi.org/10.1111/j.1469-8137.1988.tb00234.x.

Du Bay, D.T., Murdy, W.H., 1983. The impact of sulfur dioxide on plant sexual reproduction: *in vivo* and *in vitro* effects compared. J. Environ. Qual. 12, 147. https://doi.org/10.2134/jeq1983.00472425001200010027x.

Dziewięcka, M., Karpeta-Kaczmarek, J., Augustyniak, M., Majchrzycki, Ł., Augustyniak-Jabłokow, M.A., 2016. Evaluation of in vivo graphene oxide toxicity for *Acheta domesticus* in relation to nanomaterial purity and time passed from the exposure. J. Hazard Mater. 305, 30–40. https://doi.org/10.1016/j.jhazmat.2015.11.021.

Fadeel, B., Bussy, C., Merino, S., Vázquez, E., Flahaut, E., Mouchet, F., Evariste, L., Gauthier, L., Koivisto, A.J., Vogel, U., Martín, C., Delogu, L.G., Buerki-Thurnherr, T., Wick, P., Beloin-Saint-Pierre, D., Hischier, R., Pelin, M., Candotto Carniel, F., Tretiach, M., Cesca, F., Benfenati, F., Scaini, D., Ballerini, L., Kostarelos, K., Prato, M., Bianco, A., 2018. Safety assessment of graphene-based materials: focus on human health and the environment. ACS Nano 12, 10582–10620. https://doi.org/10.1021/acsnano.8b04758.

Farmer, A.M., 1993. The effects of dust on vegetation a review. Environ. Pollut. 79, 63–75. https://doi.org/10.1016/0269-7491(93)90179-R.

Fusco, L., Garrido, M., Martín, C., Sosa, S., Ponti, C., Centeno, A., Alonso, B., Zurutuza, A., Vázquez, E., Tubaro, A., Prato, M., Pelin, M., 2020. Skin irritation potential of graphene-based materials using a non-animal test. Nanoscale 12, 610–622. https://doi.org/10.1039/c9nr06815e.

Gillespie, S., Long, R., Seitz, N., Williams, N., 2014. Insecticide use in hybrid onion seed production affects pre- and postpollination processes. J. Econ. Entomol. 107, 29–37. https://doi.org/10.1603/EC13044.

Heazlewood, J.E., Wilson, S., Clark, R.J., Gracie, A., 2005. Pollination of *Vitis vinifera* L. cv. Pinot noir as influenced by *Botrytis* fungicides. Vitis - J. Grapevine Res. 44, 111–115. https://doi.org/10.5073/vitis.2005.44.111-115.

Heslop-Harrison, J., Heslop-Harrison, Y., 1970. Evaluation of pollen viability by enzymatically induced fluorescence; intracellular hydrolysis of fluorescein diacetate. Stain Technol. 45, 115–120. https://doi.org/10.3109/10520297009085351.

Hiscock, S.J., Allen, A.M., 2008. Diverse cell signalling pathways regulate pollen-stigma interactions: the search for consensus. New Phytol. 179, 286–317. https://doi.org/10.1111/j.1469-8137.2008.02457.x.

Hughes, R.N., Cox, R.M., 1994. Acidic fog and temperature effects on stigmatic receptivity in two birch species. J. Environ. Qual. 23, 686–692. https://doi.org/10.2134/jeq1994.00472425002300040010x.

Hummers, W.S., Offeman, R.E., 1958. Preparation of graphitic oxide. J. Am. Chem. Soc. 80, 1339. https://doi.org/10.1021/ja01539a017.

Joshi, K., Mazumder, B., Chattopadhyay, P., Bora, N.S., Goyary, D., Karmakar, S., 2018. Graphene family of nanomaterials: reviewing advanced applications in drug delivery and medicine. Curr. Drug Deliv. 16, 195–214. https://doi.org/10.2174/1567201815666181031162208.

Kabiri, S., Degryse, F., Tran, D.N.H., Da Silva, R.C., McLaughlin, M.J., Losic, D., 2017. Graphene oxide: a new carrier for slow release of plant micronutrients. ACS Appl. Mater. Interfaces 9, 43325–43335. https://doi.org/10.1021/acsami.7b07890.

Li, J., Jia, Y., Dong, R., Huang, R., Liu, P., Li, X., Wang, Z., Liu, G., Chen, Z., 2019. Advances in the mechanisms of plant tolerance to manganese toxicity. Int. J. Mol. Sci. 20 https://doi.org/10.3390/ijms20205096.

Liu, J., Zhao, Q., Zhang, X., 2017. Structure and slow release property of chlorpyrifos/graphene oxide-ZnAl-layered double hydroxide composite. Appl. Clay Sci. 145, 44–52. https://doi.org/10.1016/j.clay.2017.05.023.

Maguire, J.D., 1962. Speed of germination—aid in selection and evaluation for seedling emergence and vigor. Crop Sci. 2, 176–177. https://doi.org/10.2135/cropsci1962.0011183X000200020033x.

Maliyekkal, S.M., Sreeprasad, T.S., Krishnan, D., Kouser, S., Mishra, A.K., Waghmare, U. V., Pradeep, T., 2013. Graphene: a reusable substrate for unprecedented adsorption of pesticides. Small 9, 273–283. https://doi.org/10.1002/smll.201201125.

Marcano, D.C., Kosynkin, D.V., Berlin, J.M., Sinitskii, A., Sun, Z., Slesarev, A., Alemany, L.B., Lu, W., Tour, J.M., 2010. Improved synthesis of graphene oxide. ACS Nano 4, 4806–4814. https://doi.org/10.1021/nn1006368.

Mertens, Ron, 2021. The Graphene Handbook, 2021 by Ro. Ron Mertens.

Millaleo, R., Reyes-Díaz, M., Ivanov, A.G., Mora, M.L., Alberdi, M., 2010. Manganese as essential and toxic element for plants: transport, accumulation and resistance mechanisms. J. Soil Sci. Plant Nutr. 10, 476–494. https://doi.org/10.4067/s0718-95162010000200008.

Miraftab, R., Xiao, H., 2019. Feasibility and potential of graphene and its hybrids with cellulose as drug carriers : a commentary. J. Bioresour. Bioprod. 4, 200–201. https://doi.org/10.12162/jbb.v4i4.013.

Montagner, A., Bosi, S., Tenori, E., Bidussi, M., Alshatwi, A.A., Tretiach, M., Prato, M., Syrgiannis, Z., 2017. Ecotoxicological effects of graphene-based materials. 2D Mater. 4, 1–9. https://doi.org/10.1088/2053-1583/4/1/012001.

Nagajyoti, P.C., Lee, K.D., Sreekanth, T.V.M., 2010. Heavy metals, occurrence and toxicity for plants: a review. Environ. Chem. Lett. 8, 199–216. https://doi.org/10.1007/s10311-010-0297-8.

Nepi, M., Pacini, E., 1993. Pollination, pollen viability and pistil receptivity in *Cucurbita pepo*. Ann. Bot. 72, 527–536. https://doi.org/10.1006/anbo.1993.1141.

Nine, M.J., Cole, M.A., Tran, D.N.H., Losic, D., 2015. Graphene: a multipurpose material for protective coatings. J. Mater. Chem. 3, 12580–12602. https://doi.org/10.1039/C5TA01010A.

Novoselov, K.S., Geim, A.K., Morozov, S.V., Jiang, D., Zhang, Y., Dubonos, S.V., Grigorieva, I.V., Firsov, A.A., 2004. Electric field effect in atomically thin carbon films. Science 306, 666–669. https://doi.org/10.1126/science.1102896.

Novoselov, K.S., Fal'Ko, V.I., Colombo, L., Gellert, P.R., Schwab, M.G., Kim, K., 2012. A roadmap for graphene. Nature 490, 192–200. https://doi.org/10.1038/nature11458.

Oldani, K.M., Mladenov, N., Williams, M.W., Campbell, C.M., Lipson, D.A., 2017. Seasonal patterns of dry deposition at a high-elevation site in the Colorado Rocky Mountains. J. Geophys. Res. Atmos. 122, 183–200. https://doi.org/10.1002/2016JD026416.

Ou, L., Song, B., Liang, H., Liu, J., Feng, X., Deng, B., Sun, T., Shao, L., 2016. Toxicity of graphene-family nanoparticles: a general review of the origins and mechanisms. Part. Fibre Toxicol. 13, 1–24. https://doi.org/10.1186/S12989-016-0168-Y.

Pan, Y.P., Wang, Y.S., 2015. Atmospheric wet and dry deposition of trace elements at 10 sites in Northern China. Atmos. Chem. Phys. 15, 951–972. https://doi.org/10.5194/acp-15-951-2015.

Panich, A.M., Shames, A.I., Aleksenskii, A.E., Dideikin, A., 2012. Magnetic resonance evidence of manganese-graphene complexes in reduced graphene oxide. Solid State Commun. 152, 466–468. https://doi.org/10.1016/j.ssc.2012.01.005.

Petersen, E.J., Henry, T.B., Zhao, J., MacCuspie, R.I., Kirschling, T.L., Dobrovolskaia, M. A., Hackley, V., Xing, B., White, J.C., 2014. Identification and avoidance of potential artifacts and misinterpretations in nanomaterial ecotoxicity measurements. Environ. Sci. Technol. 48, 4226–4246. https://doi.org/10.1021/es4052999.

Pingue, P., Gemmi, M., Porcari, A., Alvino, A., Tombolini, F., Beltram, F., Sorba, L., Piazza, V., Ferrante, R., Boccuni, F., Lega, D., Antonini, A., Iavicoli, S., 2018. Workers' exposure to nano-objects with different dimensionalities in R&D laboratories: measurement strategy and field studies. Int. J. Mol. Sci. 19, 349. https://doi.org/10.3390/ijms19020349.

Pumera, M., Ambrosi, A., Chng, E.L.K., 2012. Impurities in graphenes and carbon nanotubes and their influence on the redox properties. Chem. Sci. 3, 3347–3355. https://doi.org/10.1039/C2SC21374E.

Qi, L., Wang, S., 2019. Sources of black carbon in the atmosphere and in snow in the Arctic. Sci. Total Environ. 691, 442–454. https://doi.org/10.1016/j.scitotenv.2019.07.073.

Rajjou, L., Belghazi, M., Catusse, J., Ogé, L., Arc, E., Godin, B., Chibani, K., Ali-Rachidi, S., Collet, B., Grappin, P., Jullien, M., Gallardo, K., Job, C., Job, D., 2011. Proteomics and posttranslational proteomics of seed dormancy and germination. In: Kermode, A. (Ed.), Seed Dormancy. Methods in Molecular Biology (Methods and Protocols). Humana Press, pp. 215–236. https://doi.org/10.1007/978-1-61779-231-1_14.

Ranal, M.A., de Santana, D.G., 2006. How and why to measure the germination process? Rev. Bras. Botânica 29, 1–11. https://doi.org/10.1590/S0100-84042006000100002.

Saladin, G., Clement, C., 2005. Physiological side effects of pesticides on non-target plants. In: Livingston, J.V. (Ed.), Agriculture and Soil Pollution: New Research. Nova Science Publisher, Inc., New York, NY, pp. 53–86.

Sawidis, T., Reiss, H.D., 1995. Effects of heavy metals on pollen tube growth and ultrastructure. Protoplasma 185, 113–122. https://doi.org/10.1007/BF01272851.

Sawidis, T., Baycu, G., Weryszko-Chmielewska, E., Sulborska, A., 2021. Impact of manganese on pollen germination and tube growth in lily. Acta Agrobot. 74, 1–17. https://doi.org/10.5586/aa.746.

Schindelin, J., Arganda-Carreras, I., Frise, E., Kaynig, V., Longair, M., Pietzsch, T., Preibisch, S., Rueden, C., Saalfeld, S., Schmid, B., Tinevez, J.-Y., White, D.J., Hartenstein, V., Eliceiri, K., Tomancak, P., Cardona, A., 2012. Fiji: an open-source platform for biological-image analysis. Nat. Methods 9, 676–682. https://doi.org/10.1038/nmeth.2019.

Shamsaei, E., de Souza, F.B., Yao, X., Benhelal, E., Akbari, A., Duan, W., 2018. Graphene-based nanosheets for stronger and more durable concrete: a review. Construct. Build. Mater. 183, 642–660. https://doi.org/10.1016/J.CONBUILDMAT.2018.06.201.

Siddiqui, M.H., Al-Whaibi, M.H., Faisal, M., Al Sahli, A.A., 2014. Nano-silicon dioxide mitigates the adverse effects of salt stress on *Cucurbita pepo* L. Environ. Toxicol. Chem. 33, 2429–2437. https://doi.org/10.1002/etc.2697.

Souza, R.H.V. de, Villela, F.A., Aumonde, T.Z., 2013. Methodologies based on seedling performance for vigor assessment of pumpkin seeds. J. Seed Sci. 35, 374–380. https://doi.org/10.1590/S2317-15372013000300015.

Speranza, A., Leopold, K., Maier, M., Rita, A., Scoccianti, V., Bo, C., 2010. Pd-nanoparticles cause increased toxicity to kiwifruit pollen compared to soluble Pd(II). Environ. Pollut. 158, 873–882. https://doi.org/10.1016/j.envpol.2009.09.022.

Speranza, A., Crinelli, R., Scoccianti, V., Taddei, A.R., Iacobucci, M., Bhattacharya, P., Ke, P.C., 2013. *In vitro* toxicity of silver nanoparticles to kiwifruit pollen exhibits peculiar traits beyond the cause of silver ion release. Environ. Pollut. 179, 258–267. https://doi.org/10.1016/j.envpol.2013.04.021.

Sun, T.Y., Gottschalk, F., Hungerbühler, K., Nowack, B., 2014. Comprehensive probabilistic modelling of environmental emissions of engineered nanomaterials. Environ. Pollut. 185, 69–76. https://doi.org/10.1016/J.ENVPOL.2013.10.004.

Sun, L., Song, H., Chang, Y., Hou, W., Zhang, Y., Li, H., Han, G., 2021. Effective removal of manganese in graphene oxide via competitive ligands and the properties of reduced graphene oxide hydrogels and films. Diam. Relat. Mater. 114, 108314 https://doi.org/10.1016/j.diamond.2021.108314.

Ter-Avanesian, D.V., 1978. The effect of varying the number of pollen grains used in fertilization. Theor. Appl. Genet. 52, 77–79. https://doi.org/10.1007/BF00281320.

Tretiach, M., Pittao, E., Crisafulli, P., Adamo, P., 2011. Influence of exposure sites on trace element enrichment in moss-bags and characterization of particles deposited on the biomonitor surface. Sci. Total Environ. 409, 822–830. https://doi.org/10.1016/j.scitotenv.2010.10.026.

Wang, X., Xie, H., Wang, Z., He, K., 2019. Graphene oxide as a pesticide delivery vector for enhancing acaricidal activity against spider mites. Colloids Surf. B Biointerfaces 173, 632–638. https://doi.org/10.1016/j.colsurfb.2018.10.010.

Waser, N.M., Price, M.V., Casco, G., Diaz, M., Morales, A.L., Solverson, J., 2017. Effects of road dust on the pollination and reproduction of wildflowers. Int. J. Plant Sci. 178, 85–93. https://doi.org/10.1086/689282.

Wetzstein, H.Y., 1990. Stigmatic surface degeneration and inhibition of pollen germination with selected pesticidal sprays during receptivity in pecan. J. Am. Soc. Hortic. Sci. 115, 656–661. https://doi.org/10.21273/JASHS.115.4.656.

Winsor, J.A., Stephenson, A.G., 1995. Demographics of pollen tube growth in *Cucurbita pepo*. Can. J. Bot. 73, 583–589. https://doi.org/10.1139/b95-061.

Winsor, J.A., Davis, L.E., Stephenson, A.G., 1987. The relationship between pollen load and fruit maturation and the effect of pollen load on offspring vigor in *Cucurbita pepo*. Am. Nat. 129, 643–656. https://doi.org/10.1086/284664.

Zanelli, D., Candotto Carniel, F., Garrido, M., Fortuna, L., Nepi, M., Cai, G., Casino, C. Del, Vázquez, E., Prato, M., Tretiach, M., 2020. Effects of few-layer graphene on the sexual reproduction of seed plants: an in vivo study with *Cucurbita pepo* L. Nanomaterials 10, 1–17. https://doi.org/10.3390/nano10091877.

Zanelli, D., Candotto Carniel, F., Tretiach, M., 2021. The interaction of graphene oxide with the pollen – stigma system : in vivo effects on the sexual reproduction of *Cucurbita pepo* L. Appl. Sci. 11, 6150. https://doi.org/10.3390/app11136150.

Zanelli, D., Candotto Carniel, F., Fortuna, L., Pavoni, E., González, V.J., Vázquez, E., Prato, M., Tretiach, M., 2022. Is airborne graphene oxide a possible hazard for the sexual reproduction of wind-pollinated plants? Sci. Total Environ. 830, 154625 https://doi.org/10.1016/j.scitotenv.2022.154625.

Zhang, L., Beede, R.H., Banuelos, G., Wallis, C.M., Ferguson, L., 2019. Dust interferes with pollen–stigma interaction and fruit set in pistachio *Pistacia vera* cv. Kerman. Hortscience 54, 1967–1971. https://doi.org/10.21273/HORTSCI14330-19.